Research Journal of Applied Sciences, Engineering and Technology 4(17): 3069-3077, 2012
ISSN: 2040-7467

Submitted: February 10, 2012 Accepted: March 12, 2012 Published: September 01, 2012

Geo Mechanical Analysis of Casing Failure in Bedded Rock Salt Formation

Tongtao Wang, Xiangzhen Yan, Xiujuan Yang, Xuewen Cao and Hongduan Huang
College of Pipeline and Civil Engineering, China University of Petroleum,
Qingdao 266580, China

Abstract: There are many bedded rock salt resources in China which are serviced as the hosts of underground natural gas storages. For the relatively thin nature of bedded rock salt and the local presence of other sedimentary rock formations, the design and safety evaluation of well completion casing take greater challenges to the engineers than that of casing in other type formations, i.e., limestone and carbonatite. The 2D and 3D geomechanical models of casing-cement sheath-rock salt are established in the paper based on the field data to obtain the creep loads in casing and find the main reasons causing casing failure. In addition, the effects of non-salt layer dip angle, friction factor between salt and non-salt layers and non-salt layer thickness, etc., on the stresses and deformations of casing are studied. The comprehensive results show hoop creep loads are the main reasons causing casing failure rather than radial creep loads. The cement sheath can improve the safety and optimize force state of casing even in perfect wellbore, which disagrees with Willson's view that the cement sheath can be neglected in a salt formation wellbore with high quality. The non-uniform factor of radial creep loads in cement sheath is slightly smaller than that of original in-situ stresses, while that of radial creep loads in casing is greatly smaller than it. The stresses and deformations of casing increase with increasing thickness of non-salt layer and decrease with the increase of friction factor. When the non-salt layer dip angle is with a value of 50 deg, the stresses and deformations achieve the max and subsequently decrease.

Keywords: Bedded rock salt, casing, creep loads, failure analysis, numerical analysis

INTRODUCTION

Many gas storage caverns are built up in the bedded rock salt formations in China (Liang *et al.*, 2007; Wang *et al.*, 2010, 2011). However, the design and safety evaluation of well completion casing take great challenges to the engineers for three main reasons. Firstly, rock salt is a typical creep material (Zhou *et al.*, 2011; Li *et al.*, 2009; Yang *et al.*, 1999), which takes place creep deformation to the wellbore under the far field in-situ stresses and causes the in-situ stresses subjected to the cement sheath and casing. Moreover, the creep loads are non-uniform in different directions. Secondly, the properties parameters of rock salt are greatly different from that of non-salt (DeVries *et al.*, 2005; Liu *et al.*, 2011), which leads the creep deformations of different layers are not accordance with each other. In this situation, the casing has to carry additional shear loads besides creep loads. Thirdly, in order to improve the efficiency of injection and production, the casing used in gas storage generally has a large dimension in diameter, which is not conducive to its security and load capacity. Once the casing of gas storage takes place failure, it will cause seriously economic losses and personal security for the highly flammable and explosive characteristic of natural gas (Thomas and Gehe, 2000). Therefore, the studies on the creep loads and failure analysis of casing in bedded rock salt formation have great engineering values.

Previous studies have shown that the creep loads in casing are mainly influenced by the initial in-situ stresses, the creep parameters of rock salt and the cement sheath quality, etc. Zhao *et al.* (2011) Hilbert and Saraf (2008) and Yang *et al.* (2006). There are two different viewpoints on the distributions of the initial in-situ stresses in available literatures. Hackney (1985), Peng *et al.* (2007), Chiotis and Vrellis (1995) and Yan *et al.* (2010) thought the initial in-situ stresses in rock salt formation were non-uniform. The casing in rock salt formation was loaded by non-uniform creep loads and the hydrostatic pressure can not be used equivalently in the casing design. However, (Li *et al*., 2009) considered the creep loads in casing were finally equal to the overburden pressure for the creep of rock salt, namely, the creep loads were uniform. Moreover, they pointed out that the non-axisymmetric deformations of casings obtained by field inspections were mainly caused by the non-uniforms of wall thickness and material, scratches and other factors, rather than the non-uniform of creep loads. Many field accidents in China have revealed the in-situ stress is not the only reason resulting in casing failure in the salt formation

Corresponding Author: Xiang Zhen Yan, College of Pipeline and Civil Engineering, China University of Petroleum, Qingdao, 266580, Shandong, China, Tel.: +86 532 86981231, Fax: +86 532 86983097

(Yang *et al*., 2006; Chen *et al*., 2009; Song *et al*., 2005). The parameters of non-salt layer also have critical effects on the casing safety. However, little attentions have been attracted.

Several methods have been conducted to calculate the creep loads in the casing in salt formations. Hackney, (1985) derived the equation of creep loads subjected to casing from the bending beam theory and validated it by the statistic casing collapse data of the Midcontinent region. He proposed the plastic strength and elastic deformation of casing should be both checked in the design of casing for salt formation. Khalaf and Cairo, (1985) presented a mathematical model based on Lame's elastic solution for thick wall cylinder to calculate the creep loads capacity of single, dual and triple casings packed with cement in salt formation. According to their results, the multiple strings and thick walled casing were superior to those of a high collapse solitary string in withstanding creep loads. Nester *et al*. (1955) obtained the failure time of casing in salt formation lasting from several weeks to more than three years from the statistic data. Through theoretical analysis and experiments, they found the wall thickness of casing in salt formation should be achieved more than two times the value of that obtained by the hydrostatic pressure design method. (Willson *et al.*, 2003) studied the magnitude and time of creep loads in well casings at the Gulf of Mexico. They pointed out that if wellbore quality can be assured, it is not always necessary to cement the casing/borehole annulus through the salt; however, if wellbore quality is poor, a cemented annulus is necessary. In fact, the existing research results (Unger and Howard, 1986; Charles and Joseph, 1986) show that the quality of a wellbore in salt formation can not be with a high level for the solution of salt into drilling fluid. Yan *et al*. (2003) built up the numerical models to obtain the creep loads in the outer surfaces of cement sheath and casing respectively. In their studies, Kelvin creep law was used to describe the creep characteristic of rock salt.

Many scholars (Munson and Wawersik, 1993; Wawersik and Zeueh, 1986; Hunsche and Albrecht, 1990) have proposed different constitutive models for the creep of rock salt. Although these models are in different forms, the actual contents are basically the same. The creep strain rate of steady creep stage can be expressed as

$$\dot{\varepsilon}(t) = K \exp\left(\frac{\Delta Q}{RT}\right).\left(\frac{\Delta \sigma}{\sigma^*}\right)^m \quad (1)$$

where, t is the creep time (s); m is the material parameter; ΔQ represents the activation energy (kJ/moL); K is the gas constant and $K = 8.3143\times10^{-3}$ kJ/(moL·K); T is the absolute temperature (K), 1ºC = 273 K; $\Delta\sigma$ stands for the deviatoric stress (MPa); σ^* indicates the normal stress (MPa), usually with a value of 1MPa.

In the study, the geomechanical models of casing in bedded rock salt formation are established. Firstly, the creep loads in casing are studied and the effects of cement sheath on casing failure are also discussed. A new failure mechanism of casing in rock salt formation is revealed. Secondly, the quantitative influences of non-salt parameters on the stresses and deformations of casing are investigated. In our investigation, rock salt is considered as a rheological material and an exponential constitutive equation is used. Encouraging results are obtained, which can provide a new failure mechanism to explain the failure and references to the design and safety evaluation of casing in rock salt.

NUMERICAL MODEL AND BOUNDARY CONDITION

The proposed salt cavern gas storage locates in Jiangsu province of China. The buried depth of objective formation where the salt cavern locates is about 1000 m below ground level. The salt cavern roof is composed by two salt layers with a non-salt layer in the middle and its thickness is about 12.5 m. The formation above the cavern roof is mudstone. For the creep of salt and changeable gas pressure, the casing in the cavern roof will be most likely failed. Therefore, it is chosen as the study target in the paper. As the casing and rock salt are consolidated together by cement, a 2D plane strain model can be used to efficiently obtain the creep loads in casing (Fig.1). In the same time, a 3D Finite Element Model (FEM) is set up based on field geological data and boundary conditions to study the effects of different parameters of non-salt layer on the casing safety (Fig. 2). The eight-node solid element SOLID45 is used in the numerical simulation, which is specialized for solving the creep deformation and highly nonlinear problem. In order to improve the accuracy and efficiency of numerical simulation, a small element size is used in near wellbore and sparser mesh is used in the distal region of the wellbore, namely, radiation grid.

Figure 1 gives the FEM to quantitatively obtain the creep loads in the casing. As we consider the symmetry of the casing, only a 1/4 model is meshed. σ_H and σ_h are the max. and min. horizontal in-situ stresses respectively. The direction of σ_H is defined with an angle of 0 deg, while σ_h is defined with an angle of 90 deg. According to the field geological data, the values of σ_H and σ_h are 27.4 and 20.6 MPa respectively. The following boundary conditions are applied: the bottom has zero vertical displacement boundaries; left side of the vertical direction has horizontal zero displacement boundaries.

Figure 2 presents the 3D FEM of casing located at the cavern roof structure with dimensions of 5×2.5×12.5 m along length, width and height direction, respectively.

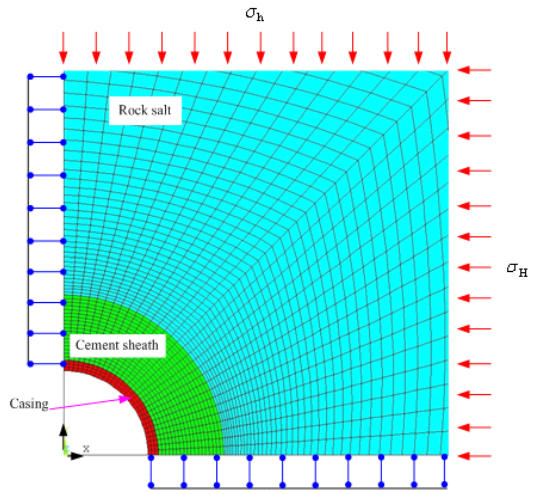

Fig. 1: 2D FEM to calculate the creep loads in casing and boundary conditions. σ_H and σ_h are the max. and min. horizontal in-situ stresses, respectively. The direction of σ_H is defined with an angle of 0 deg, while σ_h is defined with an angle of 90 deg

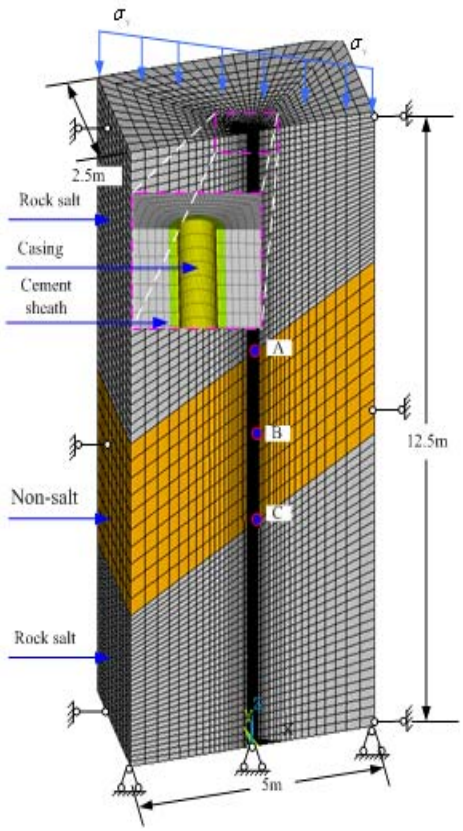

Fig. 2: 3D FEM to calculate the creep loads subjected to casing in bedded rock salt formation. A, B and C are monitoring points in the numerical simulations, which locate at the upper, middle and lower parts of non-salt layer respectively. σ_v is the vertical in-situ stress

The following boundary conditions are applied: the bottom has zero displacement boundaries, viz., the relative horizontal and vertical displacements of the model bottom are all zero under all conditions; both sides of the vertical direction have horizontal zero displacement boundaries. As the height of FEM changes slightly, the initial in-situ stresses are assigned as constants without considering the effects of in-situ stress gradient, namely, σ_H = 27.4 MPa, σ_h = 20.6 MPa and σ_v = 22.3 MPa. The other parameters used in the numerical simulations are shown in Table 1.

The whole creep process of rock salt generally can be divided into three stages, namely:

- Initial creep stage
- Stable creep stage
- Accelerated creep stage

As the underground rock salt is in the 3D in-situ stresses state, it will not take place accelerated creep except in the geologic hazard, such as earthquake. Therefore, only the first and second creep stages can take place in the actual engineering. According to (1), the creep strain rate of bedded rock salt can be calculated by $\dot{\varepsilon} = A\sigma^n$. The parameters of rock salt and non-rock salt obtained by the experiments in the numerical simulations are as follows: rock salt A = 6.0×10^{-6} $MPa^{-3.5}$/a, n = 3.5; non-rock salt A = 12.0×10^{-6} $MPa^{-3.5}$/a, n = 3.5 (Yang *et al.*, 2009).

RESULTS AND DISCUSSION

Creep loads: Figure 3 gives the radial creep loads in the outer surfaces of casing and cement sheath when the salt creep reaches the stable creep stage. The distribution of radial creep loads in cement sheath is an oval and the max. and min. radial creep loads appear in the directions of the max. and min. in-situ stresses, respectively. However, the distribution of radial creep loads in casing is an approximate circle and the max. and min. radial creep loads appear in the directions of the min. and max. in-situ stresses respectively, which are just contrary to that of cement sheath. By analyzing the casing undergauge in salt formation, it is found that the direction of undergauging deformation is accordance with the direction of the max. in-situ stress. However, the direction of the max. radial creep loads in casing obtained in the paper is opposite to that of casing undergauge. That is because the deformations of casing and cement sheath are squeezed along the max. in-situ stress direction when the creep loads subject to the cement sheath, which leads the deformation of casing along the min. in-situ stress direction extruding into the cement sheath, causing the

Table 1: Parameters used in the numerical calculations

Casing		Cement sheath		Rock salt		Non-rock salt	
OD	244.48 mm	OD	325.5 mm	Elastic modulus	14.2 Gpa	Elastic modulus	5.3 Gpa
Wall thickness	10.03 mm	Wall thickness	48.5 mm	Passion's ratio	0.31	Passion's ratio	0.27
Elastic modulus	206 Gpa	Elastic modulus	2.5 Gpa	Friction angle	39.9º	Friction angle	37.5º
Passion's ratio	0.29	Passion's ratio	0.3	Cohesion	4.36 Mpa	Cohesion	2.89 Mpa

Table 2: Max. radial creep loads in outer surfaces of casing and cement sheath and their non-uniform factors. *F* is the non-uniform factor of creep loads in cement sheath outer surface; F_i is the initial non-uniform factor of in-situ stress. The radial creep loads along the directions of the max. and min. in-situ stress are defined as σ_0 and σ_{90}, respectively.

Items	σ_0/MPa	σ_{90}/MPa	*F*	σ_H/MPa	σ_h/MPa	*Fi*
Radial creep loads in cement sheath outer surface	27.30	21.97	1.253	27.4	20.6	1.330
Radial creep loads in casing outer surface	21.79	24.97	1.146			

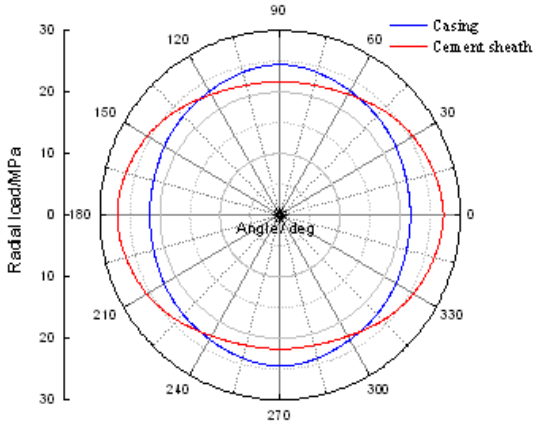

Fig. 3: Radial creep loads in outer surfaces of casing and cement sheath

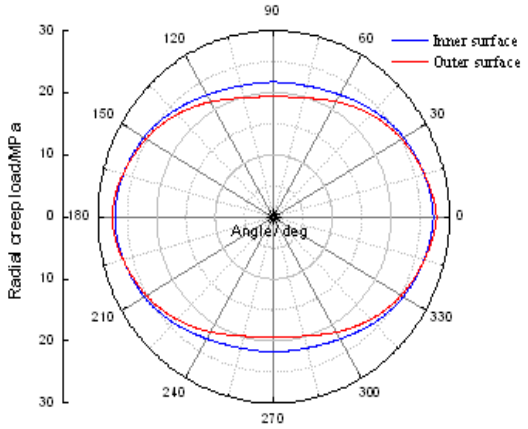

Fig. 4: Radial creep loads in inner and outer surfaces of cement sheath

increase of radial creep loads in casing. Ultimately, it causes the directions of the max. and min. radial creep loads in casing are contrary to that of in-situ stresses. The results also indicate radial creep loads are not the critical reasons causing the failure of casing in rock salt formation as the max. radial creep loads in casing do not appear in the direction of casing undergauge.

In order to compare the non-uniform of radial creep loads in the casing and cement sheath outer surfaces before and after creep, the non-uniform factor is introduced. It is the ratio of the max. and min. radial creep loads and a higher value means a stronger non-uniform of creep loads. Table 2 lists the radial creep loads and their non-uniform factors of casing and cement sheath before and after creep. By comparisons, the max. radial creep loads in cement sheath after creep are approximate equal to σ_H and the min. radial creep loads are bigger than σ_h. While the max. radial creep loads in casing are much smaller than σ_H and the min. radial creep loads are also bigger than σ_h. The non-uniform factors (*F*) of radial creep loads in the outer surfaces of casing and cement are all smaller than that of the in-situ stresses. Moreover, the *F* of radial creep loads in casing is more close to 1 as the regulation of cement sheath. It indicates the cement sheath can improve the uniform of creep loads subjected to casing and its creep loads resistance capacity. Therefore, we disagree with the viewpoint of (Willson *et al*., 2003) that the cement sheath can be neglected in a salt formation wellbore with high quality.

Figure 4 presents the radial creep loads in the inner and outer surfaces of cement sheath. The values of radial creep loads in outer and inner surfaces change slightly, showing the radial creep loads in cement sheath have little effects on the deformations and stresses of casing. Table 3 lists the final radial creep loads in wellbore inner surface, cement sheath outer and inner surfaces and casing outer surface respectively. By comparisons, cement sheath makes the radial creep loads in casing become uniform.

Figure 5 presents the relations between radial creep loads along different directions and creep times. As the increase of creep time, the radial creep loads achieve the max. and keep stable. The time of radial creep loads achieving the max. increases with increasing angle. For example, the radial creep loads with the angle of 0 deg (the max. in-situ stress direction) reach the max. needing

Table 3: Radial creep loads in wellbore inner surface, cement sheath outer/inner surface and casing outer surface

Angle/ deg	Wellbore inner surface	Cement sheath outer surface	Cement sheath inner surface	Casing outer surface
0	27.46	27.3	27.96	21.79
12	27.34	27.19	27.3	21.95
30	26.16	26.09	25.69	22.6
45	24.47	24.46	23.69	23.01
60	22.79	22.85	21.69	23.57
75	21.82	21.98	19.89	24.31
90	21.76	21.97	19.48	24.97

Table 4: Hoop creep loads in wellbore inner surface, cement sheath outer/inner surface and casing outer surface

Angle/ deg	Wellbore inner surface	Cement sheath outer surface	Cement sheath inner surface	Casing outer surface
0	25.13	24.73	22.94	224.8
12	25.49	25.25	23.56	220.9
30	25.36	25.98	24.7	212.4
45	23.87	25.28	26.35	201.3
60	22.22	24.71	28.02	190.5
75	21.93	25.67	29.32	181
90	22.67	26.65	29.84	178.9

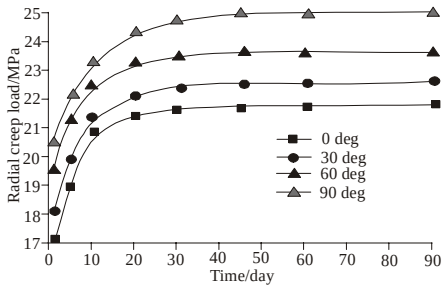

Fig. 5: Relations between radial creep loads in casing and time

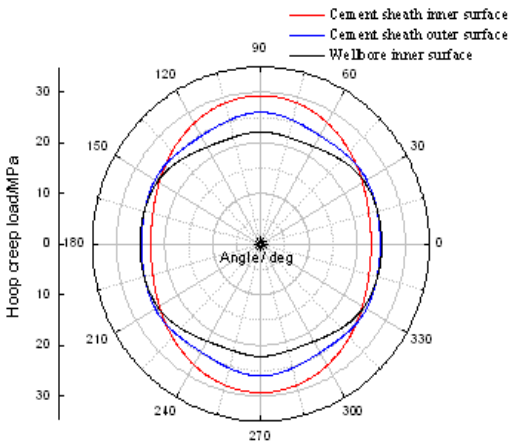

Fig. 6: Hoop creep loads in wellbore inner surface, cement sheath outer/inner surfaces

about 20 days, while that with the angle of 90 deg (the min. in-situ stress direction) reach the max. needing about 40 days under the same conditions. The values and directions of the max. and min. radial creep loads in casing are different from that of initial in-situ stresses, showing the cement sheath changes the force boundary condition of casing.

Figure 6 and Table 4 present the hoop creep loads in wellbore inner surface, cement sheath outer/inner surface and casing outer surface, respectively. The directions of the max. and min. hoop creep loads in cement sheath inner surface are opposite to that of the max. and min. in-situ stresses respectively. The non-uniform of hoop creep loads in cement sheath inner surface is much bigger than that in wellbore inner surface. When the max. hoop creep loads in wellbore inner surface exceeds the shear strength of rock salt, the well undergauge will take place along the direction of the max. in-situ stress. Subsequently, the creep loads subject to cement sheath and make it take place shear failure, also resulting in the undergauge deformation of cement sheath along the direction of the max. in-situ stress. Ultimately, the casing takes place oval deformation and the compressing and extending deformations appear in the directions of the max. and min. horizontal in-situ stresses, respectively, causing the casing extruding into cement sheath along the min. in-situ stress direction. It results in the radial creep loads becoming non-uniform seriously and the stress concentration in casing. As shown in Table 4, the max. hoop creep loads appear in the direction with angle of 90 deg (the max. in-situ stress direction), which is in accordance with the direction of casing undergauge deformation. Moreover, the values of hoop creep loads in casing are much larger than that of the radial creep loads. Therefore, the hoop creep loads are main reasons leading casing failure.

Effects of non-salt layer parameters on casing safety: For the significant differences in the properties of salt and non-salt, creep may cause the relative slide between the salt and non-salt layers and result in the shear failure of casing. Figure 7 gives the von Mises stress contours of formation and casing. The stresses of casing and formation at the intersections between salt and non-salt layers are remarkably larger than that of other locations for the stress concentration. Additionally, the stresses of salt formation are bigger than that of non-salt formation (Fig. 7a). The strength and elastic modulus of non-salt are smaller than that of rock salt and the stresses of non-salt can release easily by deformation. The relative slide between salt and non-salt layers causes the stress concentration and shear deformation of casing at the intersections (Fig. 7b). The calculating results show the casing locating at the intersections is the most vulnerable to damage and should be checked carefully in the design. Therefore, points A and C are selected as the monitoring locations in the paper to evaluate the stresses and deformations of casing and point B is a comparison point (Fig. 2).

Figure 8 presents the influences of non-salt layer dip angle on the von Mises stresses and radial deformations

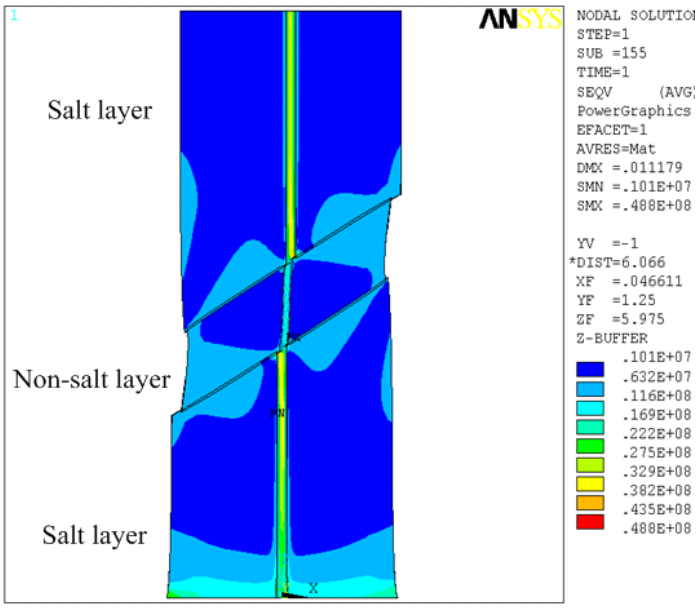

(a) Formation

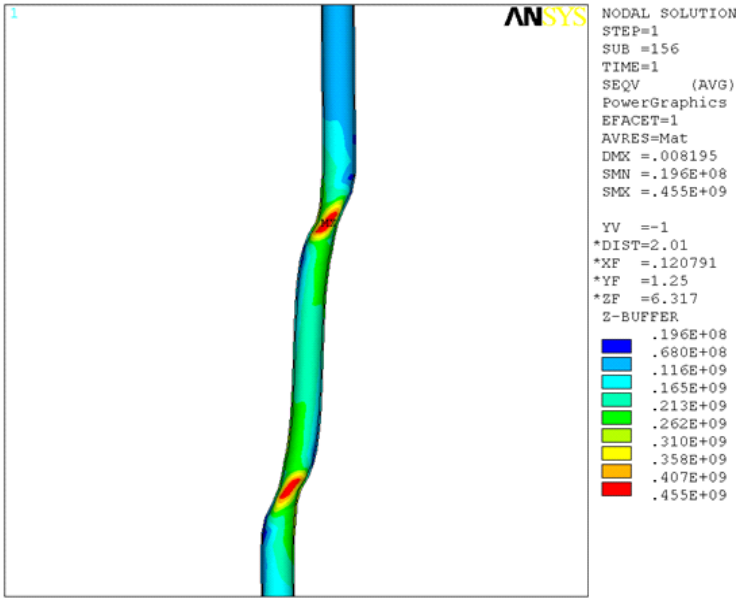

(b) Casing

Fig. 7: Von mises stress contours of formation and casing

respectively. The stresses and deformations of casing at points A, B and C increase with dip angle until it reaches about 50 deg. When the dip angle exceeds about 50 deg, the stresses and deformations reduce as the increase of dip angle. Because when the dip angle is smaller than about 50 degree, the component forces of overburden loads, self-weight and in-situ stresses along the dip direction are equidirectional with the increase of dip angle, which is subjected to the casing directly. However, when the dip angle is bigger than about 50 degree, parts of the component forces come into adjacent strata, resulting in the decrease of loads in casing. By comparisons, the non-salt layer bottom (point B) is the most dangerous location of casing, where the stresses and deformations are biggest and followed by the non-salt layer top (point A). As the weak strength and low elastic modulus of non-salt,

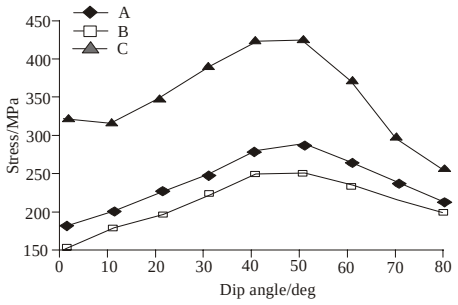

(a) von Mises stress

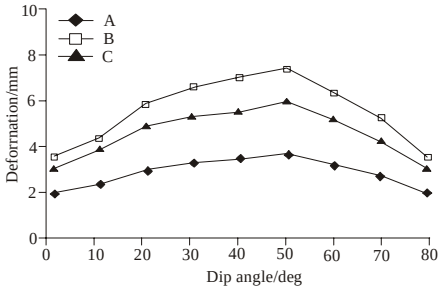

(b) Radial deformation

Fig. 8: Effects of non-salt layer dip angle on the stresses and deformations of casing for non-salt layer thickness of 2.5 m and friction factor of 0.2 case

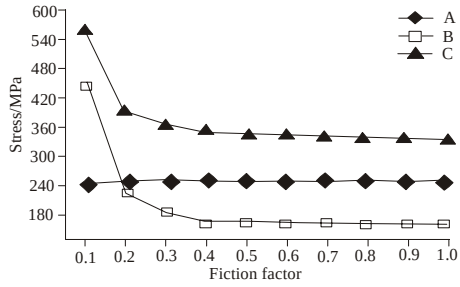

(a) von Mises stress

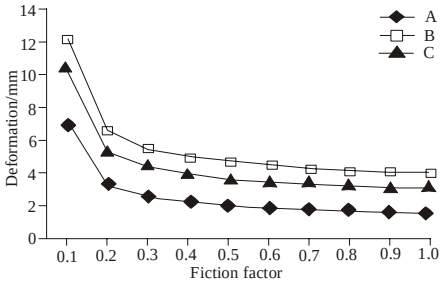

(b) Radial deformation

Fig. 9: Effects of friction factor between salt and non-salt layers on the stresses and deformations of casing for non-salt layer thickness of 2.5 m and dip angle of 30 deg case

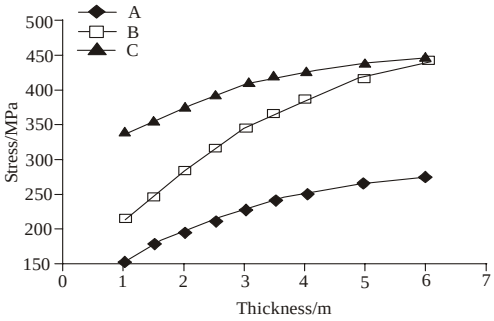

(a) von Mises stress

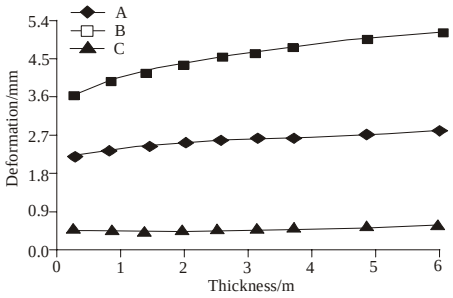

(b) Radial deformation

Fig. 10: Effects of non-salt layer thickness on the stresses and deformations of casing for dip angle of 30 deg and friction factor of 0.2 case

the loads subjected to the casing in non-salt layer are reduced by the deformations of formation. Therefore, the casing in the non-salt layer (point B) is relative safe.

Figure 9 gives the effects of friction factor between salt and non-salt layers on the stresses and deformations of casing respectively. As the increase of friction factor, the stresses and deformations reduce gradually. When the friction factor exceeds 0.5, the reduction rate becomes smooth. The shear strength of the intersection between salt and non-salt layers increases with the increasing friction factor. It improves the withstanding creep loads capacity of non-salt layer and causes the decrease of loads in casing. The calculating results also show the stresses and deformations of casing will increase significantly when the friction coefficient is low. Because once the intersection takes place failure, all the loads withstood by it are transferred to the casing.

Figure 10 illustrates the influences of non-salt layer thickness on the stresses and deformations of casing respectively. The stresses and deformations increase as the increasing thickness. Higher shear loads subjected to casing are produced in the relative slide by the non-salt layer with a bigger thickness, resulting in large stresses and deformations. For examples, when the non-salt layer with thicknesses of 1, 3 and 6 m, the von Mises stresses of casing at point A are 338.84, 410.83 and 451.62 MPa,

increased by 21.25 and 33.28% respectively. It shows a small thickness non-salt layer in the cavern roof structure is beneficial to the casing safety.

CONCLUSION

- The 2D and 3D geomechanical models of casing-cement sheath-rock salt are established based on the field data to obtain the creep loads in the casing. A new failure mechanism of casing in salt formation is revealed. The effects of non-salt layer dip angle, friction factor between salt and non-salt layers and non-salt layer thickness, etc., on the stresses and deformations of casing are given. The cement sheath can improve the safety and optimize force state of casing. We do not agree with Willson's view that the cement sheath can be neglected in a salt formation well with high quality.
- The distribution of radial creep loads in cement sheath is an oval and the max. and min. radial creep loads appear in the directions of max. and min. in-situ stresses respectively, while the max. and min. radial creep loads in casing appear in the opposite directions. The non-uniform factor of radial creep loads in casing is much smaller than that of the in-situ stress. Radial creep loads are not the main reasons causing casing failure.
- The directions of the max. and min. hoop creep loads in cement sheath inner surface are opposite to that of min. and max. in-situ stresses respectively, which aggravates the force states of wellbore, cement sheath and casing. Ultimately, this causes the undergauge deformation and failure of casing. Hoop creep loads are the direct reasons causing casing failure rather than radial creep loads.
- The stresses and deformations of casing are equidirectional with the increase of non-salt layer dip angle and thickness, but reverse to the increase of friction coefficient between salt and non-salt layers, which achieve the max. when the layer dip angle is about 50^{o} and subsequently decline.

ACKNOWLEDGMENT

The authors wish to acknowledge the financial support of China Postdoctoral Science Foundation funded project (No. 2012M511557) and Post-doctor Innovation Research Program of Shandong Province (No.201102033).

REFERENCES

Charles, A.H. and B.J. Joseph, 1986. A method for drilling moving salt formations-drilling and underreaming concurrently. SPE Drill. Eng., 8: 315-324.

Chen, Z.F., W.P. Zhu, Q.F. Di and Q.J. Zheng, 2009. Effects of cement sheath elasticity modulus and thickness on casing strength in salt beds. Petrol. Drill. Tech., 37(5): 58-61.

Chiotis, E. and G. Vrellis, 1995. Analysis of casing failure of deep geothermal wells in Greece. Geothermics, 24(5-6): 695-705.

DeVries, K.L., G.D. Callahan and K.D. Mellegard, 2005. Numerical Simulations of Natural Gas Storage Caverns in Bedded Salt. Alaska Rocks 2005, The 40th U.S. Symposium on Rock Mechanics (USRMS), June 25-29, Anchorage, AK.

Hackney, R.M., 1985. A New Approach to Casing Design for Salt Formations. SPE/IADC Drilling Conference, 5-8 March, New Orleans, Louisiana.

Hilbert, L.B. and V.K. Saraf, 2008. Salt mechanics and casing deformation in solution-mined gas storage operations. In: Proceedings of the 42nd US rock mechanics symposium, San Francisco.

Hunsche, U. and H. Albrecht, 1990. Results of true triaxial strength tests on rock salt. Eng. Fract. Mech., 35(4-5): 867-877.

Khalaf, F. and U. Cairo, 1985. Increasing casing collapse resistance against salt-induced loads. Middle East Oil Technical Conference and Exhibition, 11-14 March, Bahrain. SPE: 13712-MS.

Li, Z.F., Y.G. Zhang and X.J. Yang 2009a. Mechanics model for interaction between creep formation and oil well casing. Acta. Petrolei. Sinica., 30(1): 129-132.

Li, Y.P., C.H. Yang, J.J.K. Daemen, X.Y. Yin and F. Chen, 2009b. A new Cosserat-like constitutive model for bedded salt rocks. Int. J. Numer. Anal. Meth. Geomech., 33(15): 1691-1720.

Liang, W.C., Y. Yang, M.B. Zhao, M.B. Dusseaultc and J. Liu, 2007. Experimental investigation of mechanical properties of bedded salt rock. Int. J. Rock Mech. Min., 44(3): 400-411.

Liu, X.Y., L.J. Ma, S.N. Ma, X.W. Zhang and L. Gao, 2011. Comparative study of four failure criteria for intact bedded rock salt. Int. J. Rock Mech. Min., 48(2): 341-346.

Munson, D.E. and W. Wawersik, 1993. Constitutive Modeling of Salt Behavior State of the Technology. In: W. Wittke Balkema, (Ed.), Proceedind of 7th International Conger on Rock Mechanics Rotterdam, pp: 1797-1810.

Nester, J.H., D.R. Jenkins and R. Simon, 1955. Resistances to failure of oil well casing subjected to non-uniform transverse loading. Drill. Product. Pract., pp: 374-378.

Peng, S.P., J.T. Fu and J.C. Zhang, 2007. Borehole casing failure analysis in unconsolidated formations: A case study. J. Petrol. Sci. Eng., 59(3-4): 226-238.

Song, S.L., H.T. Wang, H.T. Ma, M. Song and X.M. Jiang, 2005. Creeping regularity of salt bed and measures for avoiding casing damage in Zhongyuan Oilfield. Acta Petrolei Sinica, 26(2): 119-122.

Thomas, R.L. and R.M. Gehe, 2000. A brief history of salt cavern use. Keynote address at salt 2000, Solution Mining Research Institute, The Hague, 7-11 May.

Unger, K.W. and D.C. Howard, 1986. Drilling techniques improve success in drilling and casing deep over thrust belt salt. SPE Drill. Eng., 6: 183-192.

Wang, T.T., X.Z. Yan, X.J. Yang and H.L. Yang, 2010. Improved Mohr-Coulomb criterion applicable to gas storage caverns in multi-laminated salt stratum. Acta. Petrolei. Sinica., 31(6): 1040-1044.

Wang, T.T., X.Z. Yan, H.L. Yang and X.J. Yang, 2011. Stability analysis of the pillars between bedded salt cavern groups by cusp catastrophe model. Sci. China Technol. Sci., 54(6): 1615-1623.

Wawersik, W.R. and D.H. Zeueh, 1986. Modeling and mechanistic interpretation of creep of rock salt below 200?. Tectonophysics, 121: 125-152.

Willson, S.M., A.F. Fossum and J.T. Fredrich, 2003. Assessment of salt loading on well casings. SPE Drill. Completion, 3: 13-21.

Yan, X.Z., H.L. Yang and X.J. Yang, 2003. The reason analysis of mudstone creep on casing damage. Drill. Prod. Technol., 26(3): 65-68.

Yan, X.Z., T.T. Wang, X.J. Yang and J.J. Wang, 2010. Improved Gauss-Newton-Marquardt algorithms for displacement back analysis of casing external loads in salt stratum. Natural Computation, 6th International Conference, YanTai, China.

Yang, C.H., J.J.K. Daemen and J.H. Yin, 1999. Experimental investigation of creep behavior of salt rock. Int. J. Rock Mech. Min. Sci., 36(2): 233-242.

Yang, H.L., M. Chen, Y. Jin and H.Z. Xiao, 2006. Study on casing dynamic loads in complex salt-bed. Petrol. Drill. Tech., 34(5): 21-23.

Yang, C.H., Y.P. Li and F. Chen, 2009. Bedded Rock Salt Mechanics and Engineering. Science Press, Beijing, pp: 179-188.

Zhao, H.F., M. Chen and J.J. Wang, 2011. Salt loading on casing in cased wellbore sections. Int. J. Rock Mech. Min., 48: 501-505.

Zhou, H.W., C.P. Wang, B.B. Han and Z.Q. Duan, 2011. A creep constitutive model for salt rock based on fractional derivatives. Int. J. Rock Mech. Min., 48: 116-121.